Biointerface Research in Applied Chemistry
Open-Access Journal (ISSN: 2069-5837)

Article
Volume 15, Issue 5, 2025, 71
https://doi.org/10.33263/BRIAC155.071

Chemical Insights into the Antiviral Mechanisms of Marine Sulfated Polysaccharides: An In-Silico Screening and Molecular Docking Study

Azalia Puspa Herida [1], Muhammad Zainuri [1,*], Hermin Pancasakti Kusumaningrum [2,*], Agus Sabdono [1], Subagiyo [1], Candra Wahyuningsih [1]

[1] Marine Science, Faculty of Fisheries and Marine Science, Diponegoro University, Prof. Jacub Rais Street, Semarang, Indonesia; azaliapuspaherida101@students.undip.ac.id (A.P.H.); muhammadzainuri@lecturer.undip.ac.id (M.Z.); agussabdono@lecturer.undip.ac.id (A.S.); subagiyo@lecturer.undip.ac.id (S.); candrawahyuningsih11@students.undip.ac.id (C.W.);
[2] Biotechnology Study Program, Department of Biology, Faculty of Science and Mathematics, Diponegoro University, Prof. Soedarto Street, Semarang, Indonesia; herminpk@live.undip.ac.id (H.P.K.);
* Correspondence: muhammadzainuri@lecturer.undip.ac.id (M.Z.); herminpk@live.undip.ac.id (H.P.K.);

Received: 20.03.2025; Accepted: 10.05.2025; Published: 10.08.2025

Abstract: In recent years, several viral diseases have emerged suddenly, leading to widespread infection and fatalities. SARS-CoV-2, which appeared in late 2019, mutates frequently, and current vaccines have limited effectiveness in fully preventing SARS-CoV-2 infections. As a result, natural antiviral medicines have gained attention, particularly sulfated polysaccharides from seaweeds, which are promising sources of bioactive compounds for antiviral activity and immune support. This study screened the types of sulfated polysaccharides, such as carrageenan, fucoidan, and ulvan, using computational analysis to evaluate their antiviral potential against SARS-CoV-2. Molecular docking was conducted to examine potential interactions with human ACE2, SARS-CoV-2's RBD, and main protease. The results of molecular docking analysis showed that kappa carrageenan exhibited better docking scores of -9.3 kcal/mol with ACE2 and -8.1 kcal/mol with spike protein-RBD. Meanwhile, carrageenan showed a better docking score of -7.6 kcal/mol with the main protease. The prediction of drug compounds based on RO5 indicates that all bioactive test compounds have the potential to be used as therapeutic agents. It is concluded that the sulfated polysaccharides derived from red seaweed, namely carrageenan and its derivatives, exhibit greater potential in demonstrating antiviral activity against SARS-CoV-2 compared to fucoidan and ulvan.

Keywords: sulfated polysaccharides; seaweeds; antiviral; SARS-CoV-2; molecular docking.

1. Introduction

COVID-19, short for Coronavirus Disease 2019, is defined by the World Health Organization (WHO) as a respiratory disease that first appeared in Wuhan, China, in late 2019. This disease originates from SARS-CoV-2 (Severe Acute Respiratory Syndrome Coronavirus 2), which is a newly identified coronavirus belonging to the Coronaviridae family [1]. SARS-CoV-2 is considered a universal concern, especially in the health sector, due to its high mortality and morbidity rates. SARS-CoV-2 is classified as a pandemic that is happening globally because it is a virus that has a high rate of spread to various countries and continents and attacks various age groups with various health conditions [2-4]. This virus can use its RNA as mRNA to synthesize viral proteins because its RNA genome is a type of positive-sense single-stranded RNA genome. The SARS-CoV-2 RNA genome is around 26-32 kilobases long and consists of several ORFs (Open Reading Frames) that are responsible for various functions. The ORF1ab gene of SARS-CoV-2 is the largest gene that encodes polyproteins and nsp12. This gene is also known as RdRp, short for RNA-dependent RNA polymerase, which is very important for viral replication. Structurally, coronavirus genes include the spike (S) gene, which encodes the S protein and functions as an intermediary for virus entry through the S1 and S2 domains; the envelope (E) gene functions as an E protein encoder; the membrane (M) gene functions as an M protein encoder; and the nucleocapsid (N) gene as the N protein encoder. In addition, SARS-CoV-2 has accessory genes such as ORF3a, ORF6, ORF7a, ORF7b, and ORF8, which produce six types of accessory proteins. This genome is located in the non-coding region in the form of 5'UTR (5' untranslated region) and 3'UTR (3' untranslated region) [5-7].

SARS-CoV-2 infection of host cells introduces the attachment of the coronavirus via its spike glycoprotein. The coronavirus spike protein mediates viral fusion and enhances the entry of the viral genome into the host cell. The spike protein comprises two subunits, namely the S1 subunit and the S2 subunit. In the S1 subunit, there is an RBD (receptor binding domain), which functions to recognize and attach to the surface receptors in the form of ACE2 (angiotensin-converting enzyme 2) on the host cell. At the same time, the S2 subunit in the spike protein is responsible for the membrane fusion process for the virus entry into the host cell [8-10]. The ORF1ab gene in SARS-CoV-2 forms two primary polyproteins, namely pp1a and pp1ab, which are also found in most of the Coronaviridae family. These polyproteins are transformed through the process of cutting the polyprotein by two proteases, namely the main protease (3Clpro) and papain-like protease (PLpro). Both proteases are responsible for cleaving and converting polyproteins into functional non-structural proteins (NSPS). Due to its essential role in viral reproduction and host-cell interaction, the main protein (Mpro) of SARS-CoV-2 is regarded as a promising target in the development of antiviral drugs to control COVID-19 [11,12]. The discovery of antiviral drugs to inhibit SARS-CoV-2 infection requires the identification of key targets. Several potential targets can be explored based on the mechanism of virus infection in host cells, including spike protein viral proteases (main protease and ACE2), which function as an early receptor for virus recognition.

The search for bioactive compounds derived from natural sources has gained popularity in developing natural products with significant roles in advancing treatments for the prevention of various diseases, particularly those caused by SARS-CoV-2. Targeted therapies enhance efficiency and minimize drug toxicity in preventing viral infections based on the unique structural properties of SARS-CoV-2. Numerous potential bioactive compound sources are being studied, with marine natural resources emerging as a promising area due to the Earth's vast aquatic ecosystems, which surpass terrestrial regions in size. Among these resources, seaweed stands out as a common and abundant source. Sulfated polysaccharides, widely found in seaweed, have been reported to possess phytopharmaceutical effects [13]. Natural products and traditional medicines are increasingly being recognized as potential alternative treatments for COVID-19 due to the limited availability of effective conventional therapies. Antiviral treatment for SARS-CoV-2 has so far been associated with drug dependency, adverse side effects, and the potential for antimicrobial resistance. One such drug is remdesivir, an antiviral approved by the U.S. FDA, though its clinical effects remain controversial. Therefore, it is crucial to determine structurally efficient antiviral compounds that are able to prevent the virus. Sulfated polysaccharides have emerged as promising bioactive compounds for alternative SARS-CoV-2 treatment due to their sustainable and abundant supply, low cytotoxicity, and cost-effectiveness. Furthermore, sulfated polysaccharides have specific antiviral abilities by disrupting the virus entry process by inhibiting the positive charge on the pathogen surface receptor located on the virus spike protein, thereby preventing the coronavirus from attaching to the host cell surface [14-17]. Sulfated polysaccharides in seaweed consist of various types depending on the seaweed group. Therefore, sulfated polysaccharide compounds sourced from seaweed are interesting candidates for the development of potential antiviral agents. This study differs from other research on sulfated polysaccharides as antiviral agents based on the source of the sulfated polysaccharides used. Research on various types of sulfated polysaccharides derived from different species of seaweed and their effects on key target proteins engaged in SARS-CoV-2 infection of host cells remains limited. This study will discuss the antiviral abilities of several types of sulfated polysaccharides (carrageenan, fucoidan, and ulvan) against SARS-CoV-2 (RBD and main protease) and the ability of sulfated polysaccharides to be used as treatment materials through computational program-based analysis. This study aims to provide a new approach to the therapeutic discovery and vaccines for the therapy of coronaviruses, especially COVID-19.

2. Materials and Methods

2.1. Protein preparation.

The structure of target proteins was collected from the protein data bank (https://www.rcsb.org) in pdf format. The target proteins were ACE2 (PDB ID: 1R42), spike protein-RBD (PDB ID: 6LZG), and main protease (PDB ID: 6LU7). The protein structure was prepared by removing unwanted molecules such as water, dimers, short bonds, and native ligands to produce a clean protein structure. The protein was transformed into PDBQT format using Biovia Discovery Studio software [18,19].

2.2. Ligand preparation.

The 3D structure of ligands was collected from PubChem (https://pubchem.ncbi.nlm.nih.gov) and ChEBI (https://www.ebi.ac.uk/chebi/) in SDF format. PubChem is a comprehensive resource library of chemical compounds and their biological activities. It is organized into three databases: substances, compounds, and bioassays [20]. The ligands were carrageenan (CID: 9907284), lambda carrageenan (ChEBI: 37167), kappa carrageenan (ChEBI: 10583), iota carrageenan (ChEBI: 37168), fucoidan (CID: 129532628), and ulvan (CID: 129692323). The ligand was transformed into PDB and PDBQT format by PyRx software for docking analysis [18].

2.3. Molecular docking.

The molecular docking studies were conducted on bioactive compounds of sulfated polysaccharides as test ligands against target proteins, namely ACE2 (human), spike-RBD protein, and main protease (SARS-CoV-2). Pyrx – Phyton Prescription 0.8 software was used in molecular docking analysis, supported by tools such as AutoDockTools, AutoDock Vina, and Open Babel. AutoDockTools was used to input files, Open Babel was used to minimize the energy of the files, and AutoDock Vina was used for docking. Test ligands and target proteins were placed on the binding site (grid box) to perform docking analysis. Molecular docking results with the lowest binding affinity energy and RMSD (Root Mean Square Deviation) confirmation value were selected, analyzed, and visualized using Biovia Discovery Studio software [18].

2.4. Lipinski's rule test.

Lipinski's rule of five (RO5) was used as a parameter for drug similarity analysis, which suggests molecular properties to determine good penetration and oral absorption capabilities. Lipinski's rule test was determined by the Super Computing Facility of Bioinformatics and Computational Biology website by entering the compound files in SDF or PDB format (http://www.scfbio-iitd.res.in/software/drugdesign/lipinski.jsp) [21,22].

3. Results and Discussion

3.1. Molecular docking.

PyRx software is used in molecular docking analysis, a computational tool for virtual drug screening. Recent research suggests that PyRx outperforms other docking software, such as AutoDock, especially in handling heterocyclic compounds. Moreover, it has demonstrated high efficiency in screening small molecules against macromolecules to identify promising drug candidates [23]. Molecular docking analysis was performed to identify potential inhibitors of SARS-CoV-2 by targeting several protein receptors derived from the virus itself and its host cells. The receptors that can be the main key targets are ACE2 (Angiotensin Converting Enzyme 2) found in humans, as well as target proteins found in viruses in the form of main protease and RBD (Receptor Binding Domain) [24]. The data on proteins, PDB IDs, and their structures used as target receptors for molecular docking are presented in Table 1.

Table 1. Receptor protein target.

Receptor name	PDB ID	Native ligand	Figure
ACE2	1R42	**2-acetamido-2-deoxy-beta-D-glucopyranose**	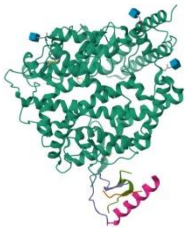
Spike protein - RBD	6LZG	2-acetamido-2-deoxy-beta-D-glucopyranose	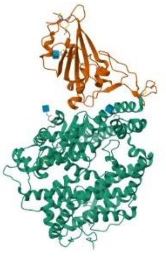

Receptor name	PDB ID	Native ligand	Figure
Main protease	6LU7	n-[(5-methylisoxazol-3-yl)carbonyl]alanyl-l-valyl-n~1~-((1r,2z)-4-(benzyloxy)-4-oxo-1-{[(3r)-2-oxopyrrolidin-3-yl]methyl}but-2-enyl)-l-leucinamide	

The target proteins, consisting of ACE2, RBD, and main protease, play an important role in the process of virus entry and replication in human host cells. Identification of various potential receptor targets can aid in identifying therapeutic targets that play a role in the development of drugs or vaccines for SARS-CoV-2. The RBD protein target is found in the spike protein, which is part of the glycoprotein that facilitates binding to the human cell receptor (ACE2) through the virus receptor (RBD). Therefore, the interaction between the ACE2 receptor and RBD holds great potential to be studied because it is responsible for the entry of the virus into human host cells. During the infection process, the ACE2 receptor will bind to the spike protein through the RBD. So, it is necessary to target the receptors found in humans and viruses to help control the interaction between host cells and viruses in managing disease development [25]. Other protein targets include the main protease. The main protease is included as an important enzyme in SARS-CoV-2, which functions to break down long polypeptide chains into functional proteins during the virus replication process. The main protease is unique to virus cells. It does not exist in human cells, making it a highly specific target for antiviral therapy without affecting normal cellular functions in the host. So, inhibiting the main protease is expected to effectively inhibit the virus replication process without affecting the replication process or normal cellular function in host cells (humans). This makes protease one of the key targets of SARS-CoV-2 antiviral therapy [26].

Identification of naturally derived bioactive compounds is widely sought to help inhibit the process of attachment and replication of the coronavirus, including the exploration of the potential of sulfated polysaccharides sourced from seaweed. The type of sulfated polysaccharides in seaweed varies depending on the seaweed group. The red seaweed group produces sulfated polysaccharides in the form of carrageenan, which can consist of lambda-carrageenan, kappa-carrageenan, and iota-carrageenan. Brown seaweed produces sulfated polysaccharides in the form of fucoidan, and the green seaweed group produces sulfated polysaccharides in the form of ulvan. These different sulfated polysaccharides exhibit distinct chemical properties and phytopharmaceutical potential [19]. Therefore, this study focuses on exploring each type of sulfated polysaccharide from various seaweed groups to identify the specific potential of bioactive compound sources for drug development.

The results of molecular docking of several target proteins and test ligands are presented, with molecular docking data expressed as binding energy (ΔG) in kcal/mol. These results explain that bioactive compounds (ligands) in the form of various types of sulfated polysaccharides can bind target proteins in humans (ACE2) and viral target proteins (RBD and main protease) with varying levels of strength. The binding energy value indicates that the bioactive compounds (ligands) tested show stable binding strength at the target protein binding site. It can be marked with a larger negative value, indicating a stronger interaction or binding affinity [19]. Testing on the human ACE2 receptor (PDB ID: 1R42), the kappa-carrageenan test ligand showed the highest binding affinity value when compared to other test ligands, control ligands, and native ligands. In addition, overall, the carrageenan group test ligands (lambda-carrageenan, kappa-carrageenan, and iota-carrageenan) showed efficient binding energy compared to the native ligand and control ligand (remdesivir). The results of molecular docking on the RBD protein target (PDB ID: 6LZG) showed that the kappa-carrageenan test ligand had the highest binding efficiency among other test ligands, followed by iota-carrageenan, which, in particular, had a higher value than the binding energy of the native ligand and control ligands. This study specifically provides new scientific insights into the ability of various sulfated polysaccharide compounds to inhibit virus attachment through two target protein sites: the target protein on human host cells (ACE2) and the target protein on viral cells (spike-RBD protein). These results specifically demonstrate the ability of kappa-carrageenan as an inhibitor of the virus attachment process to human host cells, as evidenced by the highest binding affinity values on both target proteins (ACE-2 and spike-RBD protein) [27]. The potential of kappa-carrageenan in preventing virus attachment to the host cell surface has also been reported in a molecular docking study targeting spike glycoprotein at different binding sites (PDB ID: 6VYB), where kappa-carrageenan showed the strongest binding affinity (-14.37 kcal/mol) [28]. Carrageenan exhibits antiviral properties by inhibiting viral attachment through interactions between sulfated polysaccharides and the spike protein-RBD that binds to the host cell's ACE2 receptor [29,30]. For the main protease (PDB ID: 6LU7), carrageenan test ligands demonstrated the highest binding affinities. Among these, iota-carrageenan provided efficient binding energy for the main protease compared to the control and native ligands—sulfated polysaccharides derived from red seaweed exhibit significant antiviral activity against SARS-CoV-2 and its variants. Lambda-, kappa-, and iota-carrageenan have been shown to inhibit SARS-CoV-2 replication, including variants of concern [30]. Sulfated polysaccharides, particularly the carrageenan group, exhibit inhibitory potential against viral entry, attachment, and replication based on binding affinity data. Since viral entry into host cells is a critical step in infection, preventing this mechanism enhances the effectiveness of antiviral drug discovery strategies and warrants further investigation [16]. Molecular docking serves as an essential preliminary step in identifying potential drug candidates before proceeding to in vitro and in vivo testing. Therefore, following molecular docking analysis, further in vitro and in vivo studies are necessary to validate and develop antiviral drug candidates. The results of molecular docking of several target proteins and test ligands can be seen in Table 2 and Figure 1.

Table 2. The binding energy of the ligand and receptor protein.

Receptor	Ligand	Binding affinity (kcal/mol)	Interacting amino acid residues	Bond distance
ACE2 (1R42)	Carrageenan	-8.1	SER (A:511); GLN (A:102); GLN (A:98); ALA (A:99); GLU (A:208); GLU (A:398); ASP (A:206)	3.03; 3.65; 3.32; 5.20; 2.90; 4.67; 4.24
	Lambda Carrageenan	-7.6	ASN (A:394); LYS (A:562); TRP (A:203); TYR (A:202); GLN (A:102); SER (A:511); GLU (A:398); ASN (A:397); ARG (A:514); PHE (A:400); TYR (A: 515); HIS (A:401); GLU (A:402); TYR (A: 385)	3.27; 5.55; 3.21; 4.12; 3.05; 3.26; 3.14; 2.88; 5.06; 3.15; 3.04; 3.52; 2.87; 2.75
	Kappa Carrageenan	-9.3	ARG (A:514); ARG (A:219); TYR (A:196); TRP (A:566); GLN (A:98); GLU (A:564); ALA (A:396); ASP (A:206); TYR (A: 202); GLY (A:205); TRP (A:203); GLU (A:398); SER (A:511)	5.14; 4.66; 3.09; 3.43; 3.79; 3.16; 3.13; 3.10; 4.13; 3.55; 3.27; 3.13; 3.05
	Iota Carrageenan	-9.0	ASN (A:103); HIS (A:195); ASN (A:194); GLN (A:98); LYS (A:94); GLU (A: 208); GLY (A:205); ASP (A:206); LYS (A:562);	3.11; 4.91; 3.58; 3.33; 4.36; 2.87; 3.49; 3.21; 4.32;

Receptor	Ligand	Binding affinity (kcal/mol)	Interacting amino acid residues	Bond distance
			GLN (A:102); ARG (A:219); TYR (A:196); GLN (A:81)	3.63; 4.84; 4.61; 3.07
	Fucoidan	-6.0	HIS (A:378); ALA (A:348); ARG (A:393); TYR (A:385); ASN (A:394)	3.09; 2.05; 3.07; 5.93; 3.20
	Ulvan	-4.7	GLN (A:102); ASN (A:194); HIS (A:195); GLN (A:81); GLN (A:101)	3.59; 3.66; 3.17; 2.55; 3.20
	Remdesivir	-7.9	ASP (A:382); TYR (A:385); ARG (A:514); ASP (A:350); PHE (A:40); TRP (A:349); HIS (A:378); ASN (A: 394); HIS (A:401); ALA (A:348)	2.88; 3.50; 3.29; 3.31; 4.80; 3.83; 5.16; 3.12; 3.84; 2.68
	Nafamostat	-9.0	ASP (A:350); PHE (A:40); PHE (A:390); LEU (A:73); GLN (A:102)	2.83; 4.92; 4.76; 3.85; 1.81
	Ligan Native	-6.0	ALA (A:348); ASP (A:382); HIS (A:401); ASP (A:350); TYR (A:385); ARG (A:393); PHE (A:390)	3.13; 3.07; 3.36; 3.31; 3.04; 3.11; 3.74
Spike Protein - RBD (6LZG)	Carrageenan	-6.7	SER (B:494); TYR (B:449); ARG (B:403); TYR (B:505)	2.29; 4.96; 3.20; 4.72
	Lambda Carrageenan	-6.5	GLY (B:496); GLN (B:498); TYR (B:4490; SER (B:494); TYR (B:453); ARG (B:408); GLY (B:416); LYS (B:417); GLN (B:409); ARG (B:403); TYR (B:495); TYR (B:505); PHE (B:497)	3.26; 3.00; 3.21; 3.17; 3.33; 3.17; 3.65; 2.99; 3.01; 5.12; 5.39; 5.17; 4.02
	Kappa Carrageenan	-8.1	GLN (B:498); ASN (B:501); GLY (B:496); TYR (B:495); TYR (B:453); GLU (B:406); ARG (B:403); GLN (B:409); ASP (B:405)	5.45; 3.03; 3.35; 3.79; 4.06; 3.42; 3.78; 2.81; 3.07
	Iota Carrageenan	-8.0	TYR (B:449); GLY (B:496); GLN (B:498); TYR (B:453); LYS (B:417); ARG (B:408); GLN (B:409); GLU (B:406); ARG (B:403); TYR (B:505); GLN (B:493); SER (B:494)	5.98; 318; 5.04; 3.04; 4.12; 3.04; 3.04; 2.74; 5.48; 5.48; 3.27; 3.75
	Fucoidan	-5.6	ASP (B:467); SER (B:469); GLU (B:471); LYS (B:458); ARG (B:454)	3.52; 3.03; 2.79; 3.70; 3.32
	Ulvan	-4.6	GLY (B:496); TYR (B:505)	3.20; 3.59
	Remdesivir	-6.9	SER (B:514); GLU (B:516); PRO (B:463); PRO (B:426); ASP (B:428)	3.40; 3.62; 4.57; 4.92; 3.52
	Nafamostat	-7.5	TRP (B:346); VAL (B:367); CYS (B:336); VAL (B:362)	5.90; 4.85; 2.89; 2.50
	Ligan Native	-5.6	ASN (B:354); VAL (B:341); ALA (B:348); PHE (B:347); SER (B:399); ARG (B:346)	3.22; 3.00; 3.29; 4.06; 3.11; 3.02
Main Protease (6LU7)	Carrageenan	-7.6	GLU (A:166); MET (A:165); CYS (A:145); GLY (A:143); THR (A:26)	4.09; 5.39; 5.73; 3.26; 3.02
	Lambda Carrageenan	-5.2	SER (A:1); ASN (A:214); GLY (A:2); LEU (A:282); LYS (A:5); ASP (A:216); PHE (A:3); TRP (A:207); GLU (A:288); ARG (A:4); GLY (A:283)	3.06; 2.83; 3.51; 3.57; 4.97; 5.34; 5.87; 5.56; 4.54; 3.33; 3.31
	Kappa Carrageenan	-5.6	SER (A:10); GLU (A:14); PRO (A:9); PHE (A:8); ALA (A:7); VAL (A:125); GLU (A:288); LYS (A:5)	2.97; 4.90; 3.45; 3.18; 3.19; 2.83; 3.29; 3.08;
	Iota Carrageenan	-6.7	LYS (A:5); PHE (A:3); ARG (A:4); SER (A:1); ASP (A:216); ASN (A:214); GLY (A:283); LEU (A:282)	3.12; 2.98; 3.36; 3.26; 5.36; 3.35; 3.04; 3.21
	Fucoidan	-5.3	CYS (A:145); HIS (A:41)	3.60; 4.40
	Ulvan	-4.6	GLN (A:110); ASN (A:151); PHE (A:294)	3.19; 3.19; 3.66
	Remdesivir	-6.2	LEU (A:282); GLY (A:2); PHE (A:3); ARG (A:4); LYS (A:5); GLY (A:283)	5.13; 3.67; 2.69; 3.93; 4.55; 3.69

Receptor	Ligand	Binding affinity (kcal/mol)	Interacting amino acid residues	Bond distance
	Nafamostat	-6.6	LEU (A:282); LYS (A:5); VAL (A:125); PHE (A:291); PHE (A:3)	2.92; 5.48; 2.36; 5.54; 2.61
	Ligan Native	-6.3	PHE (A:294); ASP (A:153); SER (A:158); GLN (A:110)	3.80; 3.33; 3.40; 3.05

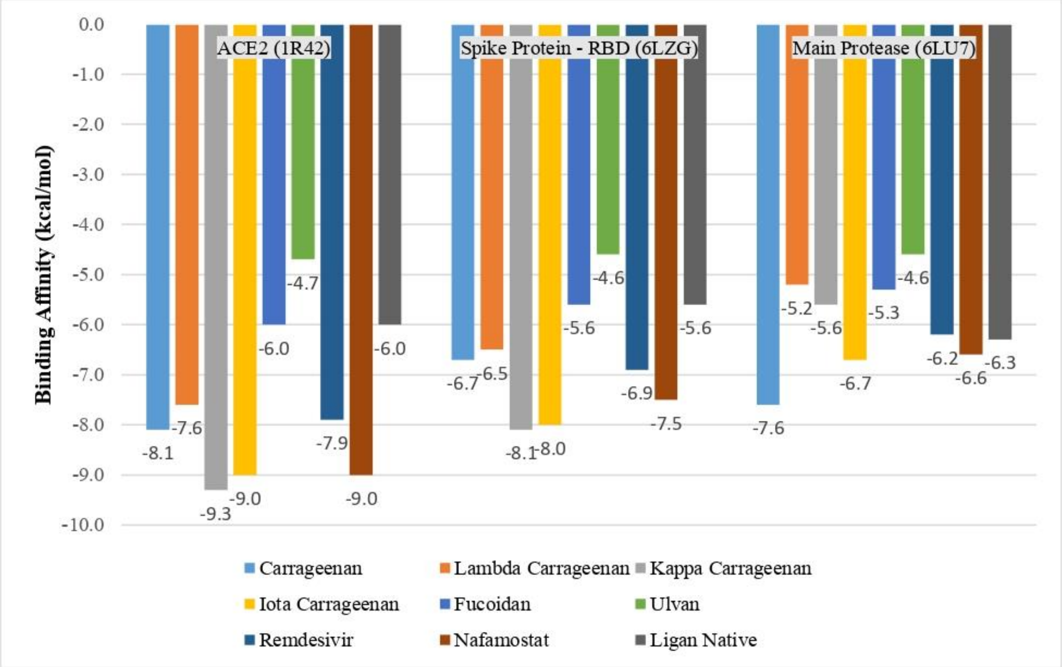

Figure 1. Docking score of ligands with ACE2 (1R42), spike protein-RBD (6LZG), and main protease (6LU7).

The results of molecular docking visualizations, as presented in Table 2, include the amino acid residue interactions and bond distances between test ligands (sulfated polysaccharides bioactive compounds), control ligands (remdesivir and nafamostat), and native ligands with their respective receptor proteins. For the ACE2 target protein, lambda-carrageenan exhibited the highest number of interacting amino acid residues (14), followed by kappa-carrageenan (13), iota-carrageenan (13), carrageenan (7), fucoidan (5), and ulvan (5). Control ligands, remdesivir and nafamostat, demonstrated 10 and 5 residue interactions, respectively, while the native ligand showed 7 interactions. The HIS (A:401) residue was consistently involved in interactions between ACE2 and lambda-carrageenan, remdesivir, and the native ligand. Similarly, for fucoidan, the residues ALA (A:348), ARG (A:393), and TYR (A:385) were found to interact with the native ligand and remdesivir.

For the spike-RBD protein, lambda-carrageenan again showed the highest number of amino acid residue interactions (13), followed by iota-carrageenan (12), kappa-carrageenan (9), fucoidan (5), carrageenan (4), and ulvan (2). The comparative ligands remdesivir, nafamostat, and the native ligand interacted with 5, 4, and 6 residues, respectively. In the case of the main protease, lambda-carrageenan displayed the most interactions (11), followed by kappa-carrageenan (8), iota-carrageenan (8), carrageenan (5), ulvan (3), and fucoidan (2). The control ligands remdesivir and nafamostat interacted with 6 and 5 residues, respectively, while the native ligand interacted with 4 residues. Key residues such as GLY (A:2), LEU (A:282), LYS (A:5), PHE (A:3), ARG (A:4), and GLY (A:283) in lambda-carrageenan were also shared with remdesivir, nafamostat, and the native ligand. Similar patterns were observed for kappa- and iota-carrageenan, indicating overlapping interactions with residues VAL (A:125), LYS (A:5), PHE (A:3), ARG (A:4), and LEU (A:282). The number of amino acid residues in the visualization of the molecular docking results that interact with the target protein on the test ligand is greater than that of the control ligand. A higher number of amino acid residues indicates an increase in the number of hydrogen bonds, which play an important role in the molecular docking interaction by strengthening the binding affinity between the protein and the ligand [31].

Comparing amino acid residues between test ligands and control or native ligands is essential for understanding protein-ligand interactions in drug design. Amino acids such as GLY, GLU, ARG, ASP, HIS, and THR are among the most conserved, making them more likely to appear in binding sites. Additionally, amino acids like TRP, HIS, MET, TYR, and PHE are abundant and capable of forming a higher number of hydrogen bonds, which enhances the stability of protein-ligand interactions. A greater number of hydrogen bonds correlates with stronger and more stable protein-ligand interactions. Additionally, hydrogen bonds that align with the interaction can validate the docking process and highlight the role of residues as catalytic sites responsible for the inhibitory activity of therapeutic agents [32-35].

Molecular interaction between target proteins (ACE2, spike protein-RBD, and main protease) and bioactive compounds with the highest binding energies, along with amino acid residue interactions, is displayed in the form of 2D visualization. The visualization serves to interpret the interaction of target proteins and test ligands for drug development. The importance of comparing amino acid residue interactions in 2D visualization to identify the location of common binding sites. Molecular docking interactions include several interaction bonds consisting of hydrogen bonds, hydrophobic interactions, and electrostatic interactions, all of which affect the strength and specificity of ligand binding to the target protein [36,37]. Furthermore, the molecular binding process, which serves as an indicator of antiviral activity, can be attributed to the distribution of negatively charged groups or the degree of sulfation present in various types of sulfated polysaccharides. Kappa-carrageenan, with a relatively low sulfation degree of one group per monosaccharide, is able to achieve stable binding at the binding site, making it reportable as bioactive against SARS-CoV-2 [19]. The 2D visualizations of molecular interactions are presented in Figure 2 and Figure 3.

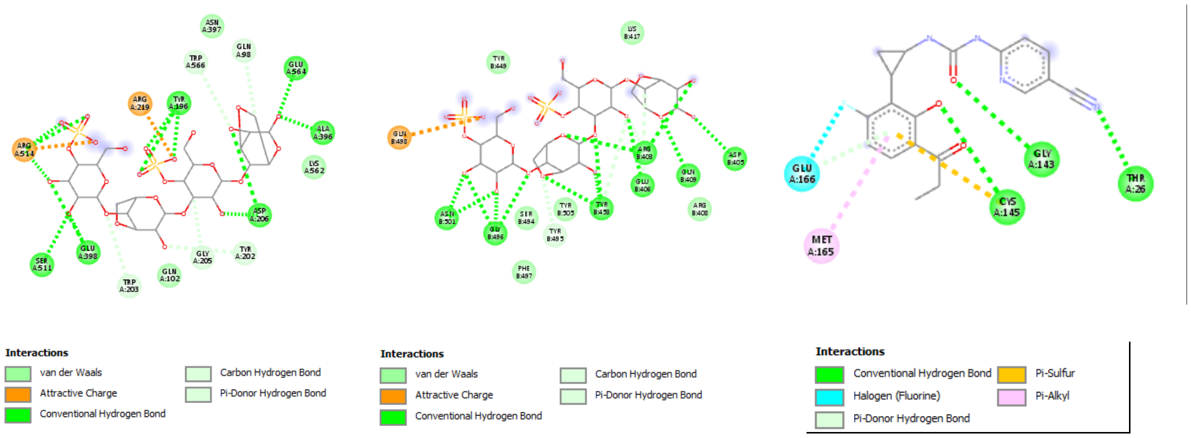

(**a**) (**b**) (**c**)

Figure 2. Visualization of ligand and receptor with the highest binding energy: (**a**) kappa-carrageenan with ACE2-1R42; (**b**) kappa-carrageenan with spike protein RBD-6LZG; (**c**) carrageenan with main protease-6LU7.

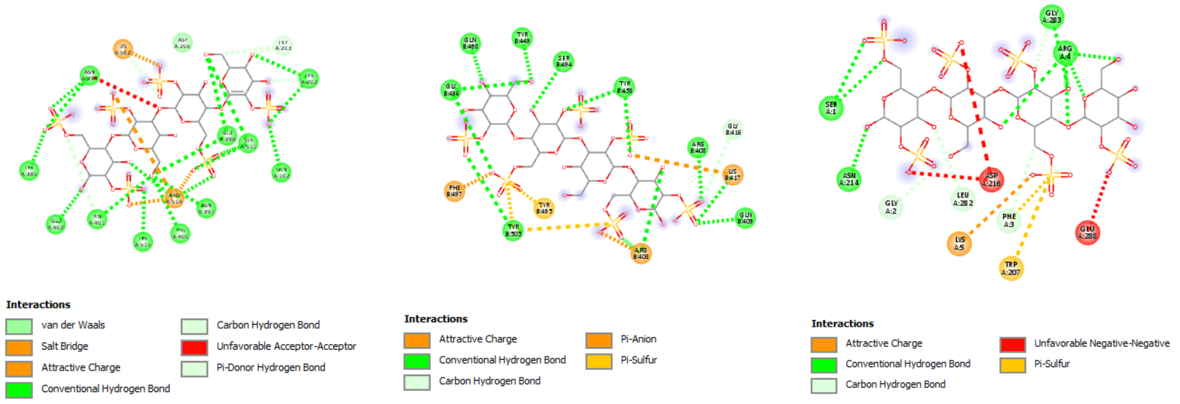

(**a**) (**b**) (**c**)

Figure 3. Visualization of ligand and receptor with the highest number of amino acid residue interactions: (**a**) lambda-carrageenan with ACE2-1R42; (**b**) lambda-carrageenan with spike protein RBD-6LZG; (**c**) lambda-carrageenan with main protease-6LU7.

Identification of natural bioactive compounds as potential candidates for COVID-19 treatment is closely linked to antiviral drugs that have been used previously. Remdesivir and nafamostat are antiviral drugs that are initial alternatives used in the treatment of SARS-CoV-2. Remdesivir is included in the antiviral drugs from adenosine analogs that have been tested on several RNA viruses, including CoV. This drug works by inhibiting the viral RdRp, which is important for virus replication. As a result, remdesivir can maximally reduce the viral load during the early stages of infection. However, being a synthetic drug, remdesivir may cause side effects, including increased liver enzymes [38,39]. Nafamostat is a nonspecific serine protease inhibitor that contains guanidino and amidino groups. Nafamostat, as an antiviral, plays a role in inhibiting the activation and invasion of human respiratory tract epithelial cells by viruses, including SARS. Therefore, this drug is considered a potential drug to prevent SARS-CoV-2 infection in host cells [40].

Sulfated polysaccharides are an alternative natural bioactive compound that offers an effective antiviral therapeutic effect with minimal side effects. Based on the results of molecular docking analysis shown in Figure 1, it is known that the interaction of sulfated polysaccharides exhibits strong binding potential to the viral replication receptor (main protease) and infection receptors (spike protein and ACE2), surpassing that of existing drugs such as remdesivir and nafamostat. This is also supported by the polyanionic properties of sulfated polysaccharides. During viral replication in host cells, sulfated polysaccharides interfere with the process of releasing the layer in the nucleoplasm and inhibit the allosteric process. In addition, the presence of sulfated polysaccharides can reduce viral protein synthesis and block the initiation of viral replication. The side effects of drug use may be mitigated by the presence of antioxidant defense and protection capabilities of these bioactive compounds. Sulfated polysaccharides possess antioxidant capabilities that help reduce the activity of free radical-producing enzymes, thereby minimizing oxidative tissue damage [16,41,42]. 3.2. Lipinski's rule of five.

Lipinski's rule of five (RO5), introduced in 1997, is an indicator for predicting drug-likeness and oral bioavailability [43]. The parameters used to predict physicochemical properties should have hydrogen bond donors less than or equal to five, hydrogen bond acceptors less than or equal to ten, molecular weight less than 500 Da, and log P of less than or equal to five. Many FDA-approved drugs or those in clinical trials have one or more RO5 parameters, particularly in classes like antiviral, antibiotics, and anticancer drugs [44,45]. The result of the screening of physicochemical properties for various types of sulfated polysaccharides can be seen in Table 3.

Table 3. Lipinski's rule test result.

Bioactive compound	Molecular weight (Da)	LogP	Hydrogen bond donor	Hydrogen bond acceptor	Molar refractivity
Carrageenan	368	3.068280	3	7	94.938675
Lambda Carrageenan	1104	-3.052619	0	39	147.461517
Kappa Carrageenan	756	-1.965170	0	25	110.101997
Iota Carrageenan	916	-1.864220	0	31	131.99751
Fucoidan	256	0.438300	2	7	53.278587
Ulvan	236	-0.605000	1	6	55.146782

In this experiment, we examined each bioactive compound proposed as a potential candidate for SARS-CoV-2 inhibitors to determine whether they meet the chemical formula, structure, and properties defined by the rule of five (RO5). Molecular weight measurements revealed that carrageenan, fucoidan, and ulvan possess molecular weights below 500 Da, indicating their potential to enhance pharmacological activity. Molecules of this size are more likely to pass through cell membranes compared to larger molecules. The log P values of all six bioactive compounds meet the criteria, with values below 5. The log P value is associated with lipophilicity, reflecting the balance of molecular distribution between lipophilic and hydrophilic phases. Higher log P values indicate increased lipophilicity, which can hinder lipid membrane penetration, reducing absorption and bioavailability [46]. The hydrogen bond donor (HBD) parameter for all bioactive compounds complies with the criteria of being below 5. Hydrogen bond donors are generally nitrogen or oxygen atoms that accept hydrogen donors that can increase the solubility of molecules in water, facilitate absorption, and improve binding to the target.

Regarding the parameters of hydrogen bond acceptors (HBA), only carrageenan, fucoidan, and ulvan meet the criteria of less than 10 acceptors. Hydrogen bond acceptors are molecules or functional groups that accept hydrogen atoms in their bonds. Excessive acceptors make the molecule overly polar, impairing membrane permeability and absorption [44]. The final parameter, molar refractivity, falls within the optimal range of 40–130 as stipulated by RO5 for carrageenan, kappa-carrageenan, fucoidan, and ulvan. While molar refractivity is not explicitly included in Lipinski's Rule of Five, it is relevant for understanding the physicochemical properties that influence solubility, permeability, and bioavailability of drug candidates [21].

4. Conclusions

This study reports that sulfated polysaccharides derived from red seaweed exhibit the ability to inhibit interactions with the ACE2 target protein (1R42), the spike protein-RBD (6LZG), and the main protease (6LU7), particularly kappa-carrageenan and lambda-carrageenan, based on binding energy values and amino acid residue interactions in molecular docking analysis. Sulfated polysaccharides such as carrageenans (lambda-, kappa-, iota-carrageenan) demonstrate potential as therapeutic molecules to control the infection and replication processes of SARS-CoV-2 in host cells (humans). Furthermore, all types of sulfated polysaccharides, including carrageenan (lambda-, kappa-, iota-carrageenan), fucoidan, and ulvan, exhibit favorable pharmacological properties and comply with the Rule of Five (RO5), indicating good absorption and bioavailability for therapeutic applications.

Author Contributions

Conceptualization, A.P.H., M.Z., and H.P.K.; methodology, A.P.H. and M.Z.; software, A.P.H. and H.P.K.; validation, A.S. and S.; formal analysis, A.P.H.; investigation, A.P.H.; resources, A.S., S., and C.W.; data curation, A.P.H.; writing—original draft preparation, A.P.H. and M.Z.; writing—review and editing, H.P.K., A.S., and S.; visualization, C.W.; supervision, M.Z. and H.P.K.; project administration, A.P.H. and C.W.; funding acquisition, M.Z. and H.P.K. All authors have read and agreed to the published version of the manuscript.

Institutional Review Board Statement

Not applicable.

Informed Consent Statement

Not applicable.

Data Availability Statement

The data of this study will be available from the corresponding author upon reasonable request.

Funding

This research was funded by DRTPM year 2024 in PDD, grant number SPK: 601-07/UN7.D2/PP/VI/2024, which is gratefully acknowledged.

Acknowledgments

We appreciate the contributions of all authors whose work was used in this article.

Conflicts of Interest

The authors declare that this research is not impacted by any competing interests.

References

1. Who. Laboratory testing for coronavirus disease 2019 (COVID-19) in suspected human cases. *Interim Guid* **2020**, 1-7.
2. Arasu, A.; Balakrishnan, P.; Velusamy, T.; Ramesh, T. Can Mandated BCG Vaccine Promote herd Immunity against Novel Coronavirus? A Potential Solution at Hand to Tackle Covid-19 Pandemic. *Curr. Immunol. Rev.* **2020,** *16*, 6–11, https://doi.org/10.2174/1573395516999201112092557.
3. Han, W.; Quan, B.; Guo, Y.; Zhang, J.; Lu, Y.; Feng, G.; Wu, Q.; Fang, F.; Cheng, L.; Jiao, N.; Li, X.; Chen, Q. The course of clinical diagnosis and treatment of a case infected with coronavirus disease 2019. *J. Med. Virol.* **2020**, *92*, 461-463, https://doi.org/10.1002/jmv.25711.
4. Dorp, L. van; Tan, C.C.; Lam, S.D.; Richard, D.; Owen, C.; Berchtold, D.; Orengo, C.; Balloux, F. Recurrent mutations in SARS-CoV-2 genomes isolated from mink point to rapid host-adaptation. *Nature Communications*. **2020**, https://doi.org/10.1038s41467-022-30698-6.
5. Khailany, R.A.; Safdar, M.; Ozaslan, M. Genomic characterization of a novel SARS-CoV-2. *Gene Rep.* **2020**, *19*, 100682, https://doi.org/10.1016/j.genrep.2020.100682.
6. Cascella, M.; Rajnik, M.; Aleem, A.; Dulebohn, S.C.; Di Napoli, R. Features, Evaluation, and Treatment of Coronavirus (COVID-19). In StatPearls; StatPearls Publishing, **2023**.
7. Zehra, Z.; Luthra, M.; Siddiqui, S.M.; Shamsi, A.; Gaur, N.A.; Islam, A. Corona virus versus existence of human on the earth: A computational and biophysical approach. *Int. J. Biol. Macromol.* **2020**, *161*, 271-281, https://doi.org/10.1016/j.ijbiomac.2020.06.007.

8. Astuti, I.; Ysrafil. Severe Acute Respiratory Syndrome Coronavirus 2 (SARS-CoV-2): An overview of viral structure and host response. *Diabetes Metab. Syndr.: Clin. Res. Rev.* **2020**, *14*, 407-412, https://doi.org/10.1016/j.dsx.2020.04.020.
9. Mittal, A.; Manjunath, K.; Ranjan, R.K.; Kaushik, S.; Kumar, S.; Verma, V. COVID-19 pandemic: Insights into structure, function, and hACE2 receptor recognition by SARS-CoV-2. *PLOS Pathog.* **2020**, *16*, e1008762, https://doi.org/10.1371/journal.ppat.1008762.
10. Zheng, J. SARS-CoV-2: an Emerging Coronavirus that Causes a Global Threat. *Int. J. Biol. Sci.* **2020**, *16*, 1678-1685, https://doi.org/10.7150/ijbs.45053.
11. Gil, C.; Ginex, T.; Maestro, I.; Nozal, V.; Barrado-Gil, L.; Cuesta-Geijo, M.Á.; Urquiza, J.; Ramírez, D.; Alonso, C.; Campillo, N.E.; Martinez, A. COVID-19: Drug Targets and Potential Treatments. *J. Med. Chem.* **2020**, *63*, 12359-12386, https://doi.org/10.1021/acs.jmedchem.0c00606.
12. Liu, P.P.; Blet, A.; Smyth, D.; Li, H. The Science Underlying COVID-19: Implications for the Cardiovascular System. *Circulation* **2020**, *142*, 68-78, https://doi.org/10.1161/CIRCULATIONAHA.120.047549.
13. Muthukumar, J.; Chidambaram, R.; Sukumaran, S. Sulfated polysaccharides and its commercial applications in food industries—A review. *J. Food Sci. Technol.* **2021**, *58*, 2453-2466, https://doi.org/10.1007/s13197-020-04837-0.
14. Shawon, J.; Akter, Z.; Hossen, M.M.; Akter, Y.; Sayeed, A.; Junaid, M.; Afrose, S.S.; Khan, M.A. Current landscape of natural products against coronaviruses: perspectives in COVID-19 treatment and antiviral mechanism. *Curr. Pharm. Des.* **2020**, *26*, 5241-5260, https://doi.org/10.2174/1381612826666201106093912.
15. Diksha, G.B.; Pai, M.O. A Compendium of Global Traditional and Alternative Medicine: An Only Alternative to Thwart the Disease in the Current Scenario of the COVID Pandemic. *Altern. Integ. Med.* **2021**.
16. Andrew, M.; Jayaraman, G. Marine sulfated polysaccharides as potential antiviral drug candidates to treat Corona Virus disease (COVID-19). *Carbohydr. Res.* **2021**, *505*, 108326, https://doi.org/10.1016/j.carres.2021.108326.
17. Mei, M.; Tan, X. Current Strategies of Antiviral Drug Discovery for COVID-19. *Front. Mol. Biosci.* **2021**, *8*, 671263, https://doi.org/10.3389/fmolb.2021.671263.
18. Dallakyan, S.; Olson, A.J. Small-Molecule Library Screening by Docking with PyRx. In Chemical Biology: Methods and Protocols, Hempel, J.E., Williams, C.H., Hong, C.C., Eds.; Springer New York: New York, NY, **2015**; Volume 1263, pp. 243-250, https://doi.org/10.1007/978-1-4939-2269-7_19.
19. Salih, A.E.M.; Thissera, B.; Yaseen, M.; Hassane, A.S.I.; El-Seedi, H.R.; Sayed, A.M.; Rateb, M.E. Marine Sulfated Polysaccharides as Promising Antiviral Agents: A Comprehensive Report and Modeling Study Focusing on SARS CoV-2. *Mar. Drugs* **2021**, *19*, 406, https://doi.org/10.3390/md19080406.
20. Salehi, S.; Abedi, A.; Balakrishnan, S.; Gholamrezanezhad, A. Coronavirus Disease 2019 (COVID-19): A Systematic Review of Imaging Findings in 919 Patients. *Am. J. Roentgenol.* **2020**, *215*, 87-93, https://doi.org/10.2214/AJR.20.23034.
21. Lipinski, C.A. Lead- and drug-like compounds: the rule-of-five revolution. *Drug Discov. Today Technol..* **2004**, *1*, 337-341, https://doi.org/10.1016/j.ddtec.2004.11.007.
22. Jayaram, B.; Singh, T.; Mukherjee, G.; Mathur, A.; Shekhar, S.; Shekhar, V. Sanjeevini: a freely accessible web-server for target directed lead molecule discovery. *BMC Bioinformatics* **2012**, *13*, S7, https://doi.org/10.1186/1471-2105-13-S17-S7.
23. Kurian, T. Molecular Docking-Based Screening of Five Heterocyclic Quinone Compounds for Antifungal Activity on Yeast Sec14p and Validation by Redocking. *J. Pharm. Res.* **2024**, *23*, 68-70, https://doi.org/10.18579/jopcr/v23.2.31.
24. Deshpande, R.R.; Tiwari, A.P.; Nyayanit, N.; Modak, M. *In silico* molecular docking analysis for repurposing therapeutics against multiple proteins from SARS-CoV-2. *Eur. J. Pharmacol.* **2020**, *886*, 173430, https://doi.org/10.1016/j.ejphar.2020.173430.
25. Wan, Y.; Shang, J.; Graham, R.; Baric, R.S.; Li, F. Receptor Recognition by the Novel Coronavirus from Wuhan: an Analysis Based on Decade-Long Structural Studies of SARS Coronavirus. *J. Virol.* **2020**, *94*, 10-1128, https://doi.org/10.1128/JVI.00127-20.
26. Zhang, L.; Lin, D.; Sun, X.; Curth, U.; Drosten, C.; Sauerhering, L.; Becker, S.; Rox, K.; Hilgenfeld, R. Crystal structure of SARS-CoV-2 main protease provides a basis for design of improved α-ketoamide inhibitors. *Science* **2020**, *368*, 409-412, https://doi.org/10.1126/science.abb3405.
27. Rohilla, D.; Srivastava, A.K.; Singh, R.P.; Yadav, P.; Singh, S.K.; Kumar, D.; Bhardwaj, N.; Kesawat, M.S.; Pandey, K.D.; Kumar, A. Algae Polysaccharides (Carrageenan and Alginate)—A Treasure-Trove of Antiviral

Compounds: An In Silico Approach to Identify Potential Candidates for Inhibition of S1-RBD Spike Protein of SARS-CoV2. *Stresses* **2023**, *3*, 555-569, https://doi.org/10.3390/stresses3030039.

28. Arunkumar, M.; Sathaiah, G.; Manikka, K.A.; Verma, M.; Patra, A.; Muniyasamy, H.; Ayyanar, S.; Balasubramaniem, A.; and Varalakshmi, P. Marine algal antagonists targeting 3CL protease and spike glycoprotein of SARS-CoV-2: a computational approach for anti-COVID-19 drug discovery. *J. Biomol. Struct. Dyn.* **2022**, *40*, 8961-8988, https://doi.org/10.1080/07391102.2021.1921032.
29. Álvarez-Viñas, M.; Souto, S.; Flórez-Fernández, N.; Torres, M.D.; Bandín, I.; Domínguez, H. Antiviral Activity of Carrageenans and Processing Implications. *Mar. Drugs* **2021**, *19*, 437, https://doi.org/10.3390/md19080437.
30. Fröba, M.; Große, M.; Setz, C.; Rauch, P.; Auth, J.; Spanaus, L.; Münch, J.; Ruetalo, N.; Schindler, M.; Morokutti-Kurz, M.; Graf, P.; Prieschl-Grassauer, E.; Grassauer, A.; Schubert, U. Iota-Carrageenan Inhibits Replication of SARS-CoV-2 and the Respective Variants of Concern Alpha, Beta, Gamma and Delta. *Int. J. Mol. Sci.* **2021**, *22*, 13202, https://doi.org/10.3390/ijms222413202.
31. Yi, C.H.; Taylor, M.L.; Ziebarth, J.D.; Wang, Y. Predictive Models and Impact of Interfacial Contacts and Amino Acids on Protein–Protein Binding Affinity. *ACS Omega* **2024**, *9*, 3454-3468, https://doi.org/10.1021/acsomega.3c06996.
32. Gallina, A.M.; Bork, P.; Bordo, D. Structural analysis of protein-ligand interactions: the binding of endogenous compounds and of synthetic drugs. *J. Mol. Recognit.* **2014**, *27*, 65-72, https://doi.org/10.1002/jmr.2332.
33. Ferreira de Freitas, R.; Schapira, M. A systematic analysis of atomic protein-ligand interactions in the PDB. *Med. Chem. Commun.* **2017**, *8*, 1970–1981, https://doi.org/10.1039/C7MD00381A.
34. Afriza, D.; Suriyah, W.H.; Ichwan, S.J.A. *In silico* analysis of molecular interactions between the anti-apoptotic protein survivin and dentatin, nordentatin, and quercetin. *J. Phys. Conf. Ser.* **2018**, *1073*, 032001, https://doi.org/10.1088/1742-6596/1073/3/032001.
35. Rai, H.; Barik, A.; Singh, Y.P.; Suresh, A.; Singh, L.; Singh, G.; Nayak, U.Y.; Dubey, V.K.; Modi, G. Molecular docking, binding mode analysis, molecular dynamics, and prediction of ADMET/toxicity properties of selective potential antiviral agents against SARS-CoV-2 main protease: an effort toward drug repurposing to combat COVID-19. *Mol. Divers.* **2021**, *25*, 1905-1927, https://doi.org/10.1007/s11030-021-10188-5.
36. Pratama, M.R.F.; Poerwono, H.; Siswodihardjo, S. Introducing a two-dimensional graph of docking score difference vs. similarity of ligand-receptor interactions. *Indones. J. Biotechnol.* **2021**, *26*, 54-60, https://doi.org/10.22146/ijbiotech.62194.
37. Agu, P.C.; Afiukwa, C.A.; Orji, O.U.; Ezeh, E.M.; Ofoke, I.H.; Ogbu, C.O.; Ugwuja, E.I.; Aja, P.M. Molecular docking as a tool for the discovery of molecular targets of nutraceuticals in diseases management. *Sci. Rep.* **2023**, *13*, 13398, https://doi.org/10.1038/s41598-023-40160-2.
38. Fauziyyah, A.; Rahmasari, R.; Sauriasari, R. The Efficacy of Remdesivir in Reducing SARS-CoV-2 Viral Load and Its Safety on COVID-19 Patients: A Systematic Review. *Jurnal Respirologi Indonesia* **2022**, *42*, 76-85, https://doi.org/10.36497/jri.v42i1.211.
39. Frediansyah, A.; Nainu, F.; Dhama, K.; Mudatsir, M.; Harapan, H. Remdesivir and its antiviral activity against COVID-19: A systematic review. *Clin. Epidemiol. Glob. Health* **2021**, *9*, 123-127, https://doi.org/10.1016/j.cegh.2020.07.011.
40. Hoffmann, M.; Schroeder, S.; Kleine-Weber, H.; Müller, M.A.; Drosten, C.; Pöhlmann, S. Nafamostat Mesylate Blocks Activation of SARS-CoV-2: New Treatment Option for COVID-19. *Antimicrob. Agents Chemother.* **2020**, *64*, 10-1128, https://doi.org/10.1128/aac.00754-20.
41. Reshi, M.L.; Su, Y.-C.; Hong, J.-R. RNA Viruses: ROS-Mediated Cell Death. *Int. J. Cell Biol.* **2014**, *2014*, 467452, https://doi.org/10.1155/2014/467452.
42. Shi, Q.; Wang, A.; Lu, Z.; Qin, C.; Hu, J.; Yin, J. Overview on the antiviral activities and mechanisms of marine polysaccharides from seaweeds. *Carbohydr. Res.* **2017**, *453-454*, 1-9, https://doi.org/10.1016/j.carres.2017.10.020.
43. Baell, J.B.; Congreve, M.; Leeson, P.; Abad-Zapatero, C. Ask the Experts: Past, Present and Future of the Rule of Five. *Future Med. Chem.* **2013**, *5*, 745-752, https://doi.org/10.4155/fmc.13.61.
44. Pollastri, M.P. Overview on the Rule of Five. *Curr. Protoc. Pharmacol.* **2010**, *49*, 9.12.1-9.12.8, https://doi.org/10.1002/0471141755.ph0912s49.

45. Lohit, N.; Singh, A.K.; Kumar, A.; Singh, H.; Yadav, J.P.; Singh, K.; Kumar, P. Description and in silico ADME studies of US-FDA approved drugs or drugs under clinical trial which violate the Lipinski's rule of 5. *Lett. Drug Des. Discov.* **2024**, *21*, 1334-1358, https://doi.org/10.2174/1570180820666230224112505.
46. Möbitz, H. Design Principles for Balancing Lipophilicity and Permeability in beyond Rule of 5 Space.*ChemMedChem.* **2024**, *19*, e202300395, https://doi.org/10.1002/cmdc.202300395.

Publisher's Note & Disclaimer